Polymer 164 (2019) 174–182

Contents lists available at ScienceDirect

Polymer

journal homepage: www.elsevier.com/locate/polymer

The effect of boehmite nanoparticles (γ-AlOOH) on nanomechanical and thermomechanical properties correlated to crosslinking density of epoxy

Media Ghasem Zadeh Khorasani[a,b,*], Dorothee Silbernagl[a], Paulina Szymoniak[a,b], Vasile-Dan Hodoroaba[a], Heinz Sturm[a,b]

[a] Bundesanstalt für Materialforschung und -prüfung (BAM), D-12205, Berlin, Germany
[b] Technical University Berlin, D-10587, Berlin, Germany

HIGHLIGHTS

- Boehmite nanoparticles enhance the properties of epoxy by inducing structural changes and alteration of network architecture of epoxy matrix.
- High resolution ImAFM force measurements revealed a significant stiffening effect of boehmite nanoparticles on epoxy matrix.
- High contents of boehmite nanoparticles results in decrease of crosslinking density, meanwhile the stiffness of the nanocomposite is improved.

ARTICLE INFO

Keywords:
Boehmite nanoparticles
Epoxy resin
Nanomechanical properties
Atomic force microscopy
Intermodulation
Crosslinking density

ABSTRACT

We show that complex physical and chemical interactions between boehmite nanoparticles and epoxy drastically affect matrix properties, which in the future will provide tuning of material properties for further optimization in applications from automotive to aerospace. We utilize intermodulation atomic force microscopy (ImAFM) for probing local stiffness of both particles and polymer matrix. Stiff particles are expected to increase total stiffness of nanocomposites and the stiffness of polymer should remain unchanged. However, ImAFM revealed that stiffness of matrix in epoxy/boehmite nanocomposite is significantly higher than unfilled epoxy. The stiffening effect of the boehmite on epoxy also depends on the particle concentration. To understand the mechanism behind property alteration induced by boehmite nanoparticles, network architecture is investigated using dynamic mechanical thermal analysis (DMTA). It was revealed that although with 15 wt% boehmite nanoparticles the modulus at glassy state increases, crosslinking density of epoxy for this composition is drastically low.

1. Introduction

Epoxy resins are well-known for their excellent mechanical properties and being especially good adhesives. Therefore, they are used as matrix in fiber-reinforced composite material for applications such as light-weight construction material [1]. The most important commercially available epoxy resin is diglycidyl ether of bisphenol A (DGEBA). Primary amines and anhydrides are typically used as curing agent [2]. Depending on the final application, the curing agent type, its ratio to the epoxy and the curing time and temperature are varied to reach the optimum mechanical performance. The main challenge with epoxy is the inherent brittleness and low fracture toughness [3]. Boehmite nanoparticles (BNP) are potential candidates to improve the fracture toughness of epoxy while enhancing its modulus at room temperature. The effect of BNPs on a large group of polymers has been already studied [4]. Previous studies report the reinforcing effect of BNPs on epoxy such as increase of shear strength, shear modulus and compressive strength while improving the fracture toughness [5–10]. Jux and coworkers demonstrated that the degree of such enhancements depends strongly on particle concentration. They reported an increase of 26% in tensile modulus and 62% in fracture toughness with adding 15 wt% BNPs to epoxy [7]. Arlt reported a decrease in glass transition temperature (T_g) of epoxy with increasing BNP concentration and suggested that curing is sterically hindered by BNPs, which results in decrease of crosslinking density in cured epoxy [5]. An in-depth investigation on network density and nanomechanical properties of composite phases is still needed to prove these mechanisms.

Recent works in polymer nanocomposites demonstrated that particles, even in low mass fractions, can result in alteration of bulk polymer properties [11]. It is generally accepted that T_g attributes to molecular

* Corresponding author. Bundesanstalt für Materialforschung und -prüfung (BAM), D-12205, Berlin, Germany.
E-mail address: media.ghasem-zadeh-khorasani@bam.de (M. Ghasem Zadeh Khorasani).

https://doi.org/10.1016/j.polymer.2018.12.054
Received 7 September 2018; Received in revised form 6 December 2018; Accepted 30 December 2018
Available online 02 January 2019

mobility. The increase in crosslinking density results in decrease of mobility of chain segments between crosslinks and results in increase of T_g. A simple approximation of network architecture is based on rubbery-like elasticity theory which correlates the crosslinking density to the storage modulus in rubbery state [12]. In thermoplastic nanocomposites, T_g shifts are usually contributed to formation of an interphase [13]. However, in nanocomposites with thermosetting matrices, particularly with crosslinked epoxies, the average crosslinking density can be influenced due to the effect of nanoparticles on chemistry of curing. In this case, the effect of particles is no longer limited to the nearest polymer layer (interphase) and thus, the bulk alteration of the matrix becomes a dominant effect.

Depending on their physical and chemical properties, nanoparticles can alter the chemistry of curing which results in either decrease or increase of crosslinking density and network homogeneity of the matrix. Here are some examples on the effect of various nanoparticles on epoxy systems: a study has shown that iron particles affect the curing kinetics of epoxy matrix and result in increase of the crosslinking density [14]. Other studies on modified carbon nanotubes have revealed a significant increase in the shear modulus of epoxy above and below T_g as a result of increased crosslinking density [15,16]. Nevertheless, contradictory results were reported from studies on silica-based particles in epoxy. One study has demonstrated that despite of improvement in elastic modulus, the bulk network structure of epoxy shows regulation by integration of silica resulting in looser network compared to neat epoxy [17]. On the other hand, another study on layered silicate-epoxy nanocomposites suggested the participation of particles in curing reaction which leads to increase of crosslinking density of the epoxy [18].

The aim of the present work is to investigate the effect of boehmite nanoparticles on the nanostructure, local stiffness and crosslinking density of epoxy system. Understanding the nanostructure of epoxy/boehmite nanocomposites can be achieved by performing high resolution AFM-based force measurements, characterizing not only the morphology but also local mechanical properties. Intermodulation AFM (ImAFM) - a multi-frequency dynamic method - provides us with quantitative force measurements with nanoscale resolution [19]. Dynamic mechanical thermal analysis (DMTA) provides us with information about the crosslinking density of the epoxy matrix. The low strain modulus in glassy state is correlated to the stiffness values obtained from ImAFM while mechanical properties at temperatures above T_g are related to network architecture of epoxy matrix. In conclusion, we suggest a complementary mechanism to the hypotheses presented in work of others.

2. Experimental

2.1. Material

The epoxy system used in this study is bisphenol-A-diglycidyl ether (DGEBA, Araldite® LY 556, Huntsman) cured with an anhydride curing agent, methyl tetrahydrophtalic acid anhydride (MTHPA, Aradur® HY 917, Huntsman) and accelerated by an amine, 1-methyl-imidazole (DY070, Huntsman). The mixture of epoxy, hardener and accelerator is 100:90:1 parts per weight, respectively. Commercially available spray dried boehmite nanoparticles with orthorhombic shape and primary particle size of 14 nm (DISPERAL HP14, SASOL, Germany) were used. Fankhänel and coworkers have determined the experimental average elastic modulus of boehmite to be approx. 10 GPa [20]. With respect to the plane orientation, this value can show deviations from the average value. Suspensions of 30 wt% BNP are blended with DGEBA and diluted with DGEBA to reach certain weight percentiles (0, 2.5, 5, 10, 15 wt%). Mixtures are cured for 4 h at 80 °C to reach gelation and 4 h at 120 °C for post-curing as suggested by the manufacturer to obtain a fully cured system.

For all measurements in this study, cured nanocomposite samples were prepared by the German Aerospace Center (DLR, Braunschweig, Germany). Details about particle dispersion and curing process of the samples used in this study are described in detail elsewhere [6,7] Here, the anhydride-cured epoxy DGEBA/MTHPA/DY070 with the mixing ratio of 100:90:1 are named as EP, and the nanocomposites as EP/BNPx (x corresponds to the weight percentage of BNPs).

2.2. Methods

All AFM measurements (tapping mode and ImAFM) were conducted with an MFP-3D AFM (Asylum Research, Santa Barbara, CA). The AFM probe used is Mikromasch, HQ:NSC35 (Wetzlar, Germany). Here we implemented a lock-in amplifier and a software designed by Intermodulation Products (Sagersta, Sweden) added to the MFP-3D AFM setup to perform dynamic force curves (Amplitude-dependence force spectroscopy- ADFS). For the analysis of ADFS curves and creating stiffness images we used software developed in our group. The resonance frequency and spring constant of the cantilever are determined by non-invasive thermal noise method [21]. The cantilever used in this study has a spring constant k_c of 13 N/m, resonance frequency ω_0 of 202 kHz and tip radius R of approx. 23 nm. Surface polishing and plasma cleaning were carried out to prepare the surface of samples for AFM measurements.

In ImAFM mode, the cantilever is driven by two frequencies above and below its resonance, $\omega_0 \pm 0.5$ kHz. As a result, the movement of the cantilever contains both frequencies leading to a beating waveform of the amplitude. When engaged with the surface, the linear response of a freely ocsillating cantilever is distorted due to the non-linear tip-surface interaction and two frequencies mix with each other (intermodulation) which yields responses at new frequencies. These responses which are called intermodulation products (IMP) are collected using a multi-frequency lock-in amplifier. For each image pixel within the scan in X and Y directions, the amplitudes and phase shifts of each IMP frequency comb are extracted by Fourier transformation of the oscillating deflection. Since the amplitude of the oscillation is directly correlated to the force, two force quadrature curves with dependency on amplitude can be constructed: 1) in-phase with the cantilever's motion which is conservative and describes the elastic behavior of the material. 2) out-of-phase which describes the dissipative forces. Amplitude-dependence force spectroscopy (ADFS) curves obtained from the conservative part of tip-surface force can be treated as conventional force-distance curves (FDC) [19,22].

Dynamic thermal mechanical analysis (DMTA) spectra were recorded using a ATM3 torsion pendulum (Myrenne, Roetgen, Germany). In this method a clamped sample is loaded with an oscillating pendulum. The sinusoidal shear deformation induces a free oscillation of the pendulum at frequency of 1 Hz with 1° strain. The measured oscillation period and damping are used to calculate the complex modulus G^*. The storage and loss moduli, G' and G'' are determined as a function of temperature. In this work, the temperature is ramped up from 20 to 200 °C with the heating rate of 1 K/min. The maximum temperature 200 °C was chosen carefully to avoid any degradation (see thermogravimentric analysis in supplementary data, SM4). The measurement is carried with the presence of nitrogen gas in the chamber. DMTA torsion pendulum was chosen over other DMTA modes (e.g. three-point bending or compression) due to high sensitivity and applying low strain which allows to stay in the linear regime through the entire measurement. DMTA measurements are carried out on epoxy samples containing 0, 1, 2.5, 5, 10 and 15 wt% BNP content. Sample dimensions were 32 mm × 5 mm × 1 mm. Each sample was measured through first heating up (first run), cooling down and second heating up (second run). Both heating cycles are further evaluated.

Thermogravimetric analysis (TGA) was performed using a STA7000 Series Thermogravimetric Analyzer (Hitachi, Chidoya, Japan), employed with a horizontal dual balance beam, enabling a microgram-level weight change detection. Samples of 8–13 mg were heated in

alumina pans from room temperature up to 1000 °C at a heating rate of 10 °C min^{-1}. Nitrogen was used as a purge gas up to approximately 600 °C to avoid oxidation reactions, thus ensuring that the sample reacts only to temperature during decompositions. At temperatures from 600 to 1000 °C, above standard pyrolysis temperatures, oxygen was used in order to oxidize the remaining pyrolytic char.

The spatial distribution of BNPs in EP/BNP15 was investigated by scanning electron microscopy (SEM) using a Zeiss Supra 40 microscope (Zeiss, Germany) equipped with a high-resolution cathode of Schottky type and conventional Everhart-Thornley (ET) and In-Lens secondary electron (SE) detectors. For better observation of the nanoparticles in the sample volume, the SEM was operated in the transmission mode, i.e. the so-called T-SEM mode [23], which offers a superior material contrast. For this purpose, free-standing 100 nm thin sections of EP/BNP15 were prepared by ultramicrotomy and deposited carefully on typical carbon TEM grid. It was not necessary to apply a conductive thin layer onto the microtome-cut sections, as they were sufficiently electrically conductive.

3. Results

The spatial distribution of BNPs in epoxy was evaluated from T-SEM micrographs as exemplary presented in Fig. 1. First, it must be noticed that the high-resolution T-SEM allows the (expected) identification of individual embedded primary nanoparticles of 14 nm. Application of high-resolution, surface-sensitive SEM with the InLens detector is confronted with the problem to distinguish clearly the buried nanostructures from potential morphological artifacts at the sample surface. Based on the T-SEM images, besides a few larger agglomerates, the overall distribution of the nanoparticles within the matrix can be considered as homogeneous. Particles mainly form agglomerates in the range of 100–200 nm size and single particles with the primary size of 14 nm are only rarely recognized.

Tapping mode AFM topography images of different scanned sizes of EP/BNP15 are presented in Fig. 2a and b. Here, the morphology of agglomerates and distribution of the particles are similar to those observed by T-SEM. Here, besides the topography, a compositional contrast is also required to distinguish between particles and other topographical artifacts due surface contamination or the well-known nodular morphology of epoxy matrix [24,25]. Thus, we consider the oscillation phase contrast to verify the location of particles as for a small scanned area presented in Fig. 2.c. This area is further evaluated by ImAFM.

3.1. Intermodulation AFM

For probing the mechanical properties of each component of the nanocomposite separately, the scan size for ImAFM needs to be small and carefully selected to include both small particles and areas of undisturbed matrix. From each pixel of the ImAFM scanned area, an ADFS force curve is obtained which can be treated similar to conventional force-distance curves. The slope of the curve in the repulsive regime is correlated to the stiffness and the area of net attractive regime corresponds to attractive forces (mainly Van der Waals) between the tip and the sample. In addition to topography image, the work of attractive force W_{attr} is used as an additional channel to precisely locate the particles and separate their force curves from force curves of matrix. The maps of stiffness and W_{attr} together with corresponding topography of the scanned area of EP/BNP15 are shown in supplementary material (SM1.1). Here we only focus on two main components of the nanocomposite, particles and matrix. In-depth investigations on interphase properties include more complex analysis of ImAFM data which will be published elsewhere [26].

Fig. 3 presents the stiffness histograms of bulk matrix and BNPs separated from the overall stiffness histogram of the scanned area in EP/BNP15. The scanned points from which the stiffness values are taken, are shown in colored pixels in the 3-D topography inset image of Fig. 3. Surprisingly, the stiffness values corresponding to epoxy are higher than of BNPs. To investigate this effect, the stiffness of neat epoxy and other concentrations requires be determined using the similar approach and compared to EP/BNP15. The lowest concentration that we could reliably locate nanoparticles with the scanned volume is 2.5 wt%. Below this concentration spotting the nanoparticles is very challenging. Since the scanned areas by ImAFM have typically a size of below 500 × 500 nm, the particle concentration varies extremely in such an area, as can be seen for example in Fig. 1. Thus, it is not possible to distinguish the effect of particle content between 2.5 or 5 and 10 or 15 wt% respectively from a local effect. Therefore, systematic study of changes in concentration is only possible with comparing two extremes of concentrations, here 0, 2.5 and 15 wt%. Topography, map

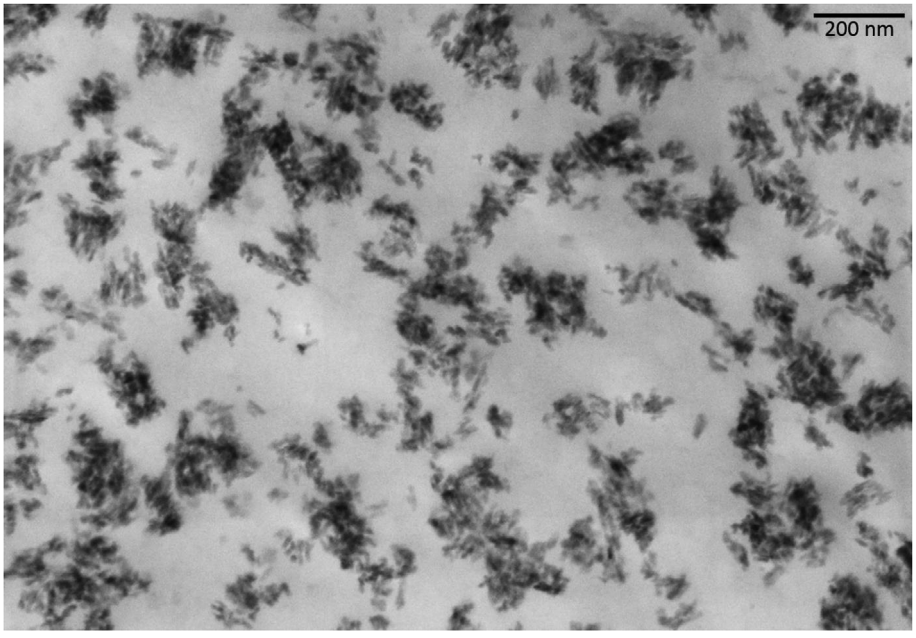

Fig. 1. 20 kV T-SEM micrograph of BNPs in anhydride-cured epoxy prepared as ultramicrotomed section.

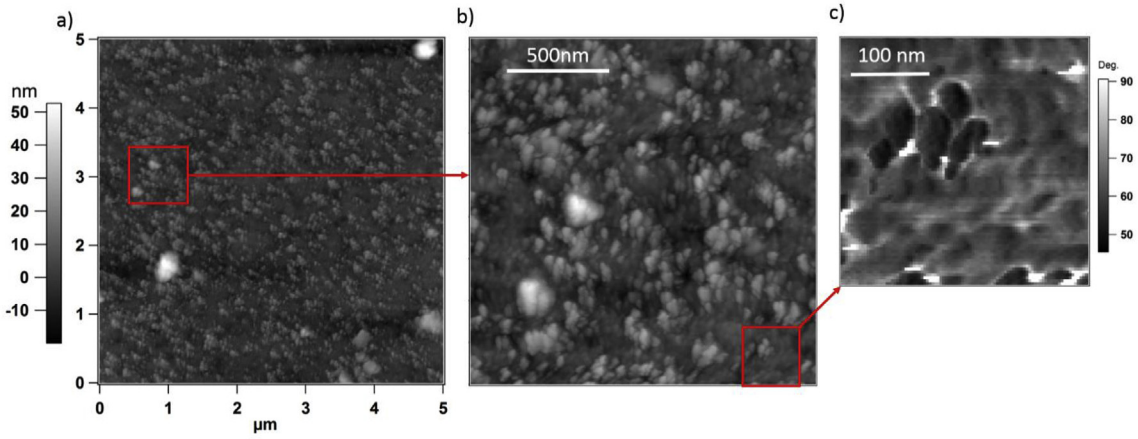

Fig. 2. a) and b) tapping mode AFM topography and c) phase image of anhydride/cured epoxy with 15wt% boehmite nanoparticles(EP/BNP15).

of stiffness and W_{attr} for EP/BNP2.5 and EP are presented in supplementary material (SM1.2 and SM1.3), respectively.

In Fig. 4, the stiffness values related to bulk epoxy in EP, EP/BNP2.5 and EP/BNP15 are presented. This comparison clearly shows the stiffening effect of boehmite on the bulk epoxy matrix which increases with increasing particle content. The stiffness of neat epoxy is considerably lower than of BNPs as expected from the initial Young's modulus values of epoxy (3.3 GPa [7]) and boehmite (10 GPa [20]). However, the stiffness of epoxy increases with introducing BNPs. The stiffening effect of nanoparticles on crosslinked matrices have been previously reported [27]. Huang and coworkers demonstrated that the bulk PDMS in the presence of silica particles has a higher stiffness compared to that of neat PDMS. However, in our study, the stiffening effect of BNPS on epoxy matrix at high particle concentration (here, with 15 wt% BNP) is in such an extent that local stiffness value of epoxy exceeds the stiffness of BNP particles, results in an inversed composite property. In this case, BNPs act as plasticizers in a highly stiff epoxy matrix. It is noteworthy that despite of increase in maximum stiffness values of epoxy matrix, the width of the stiffness distribution (the error bar in inset image of Fig. 4) increases with increasing particle concentration. This implies that although the overall stiffness is increasing, the epoxy matrix in the presence of high concentrations of boehmite exhibits a more heterogeneous behavior compared to neat epoxy. Heterogeneities are known to help dissipating energy and prevent crack propagation and brittle fracture. The increase of fracture toughness with increasing BNP concentration in composite system similar to this study has been e reported elsewhere [7].

An important remark on the stiffening effect of boehmite on epoxy, is that the Young's modulus of epoxy matrix is changed accordingly and therefore the assumption from previous studies that the increase in the modulus of elasticity is exclusively due to the contribution of particle modulus must be revised [5,7,9]. Considering that the Young's modulus

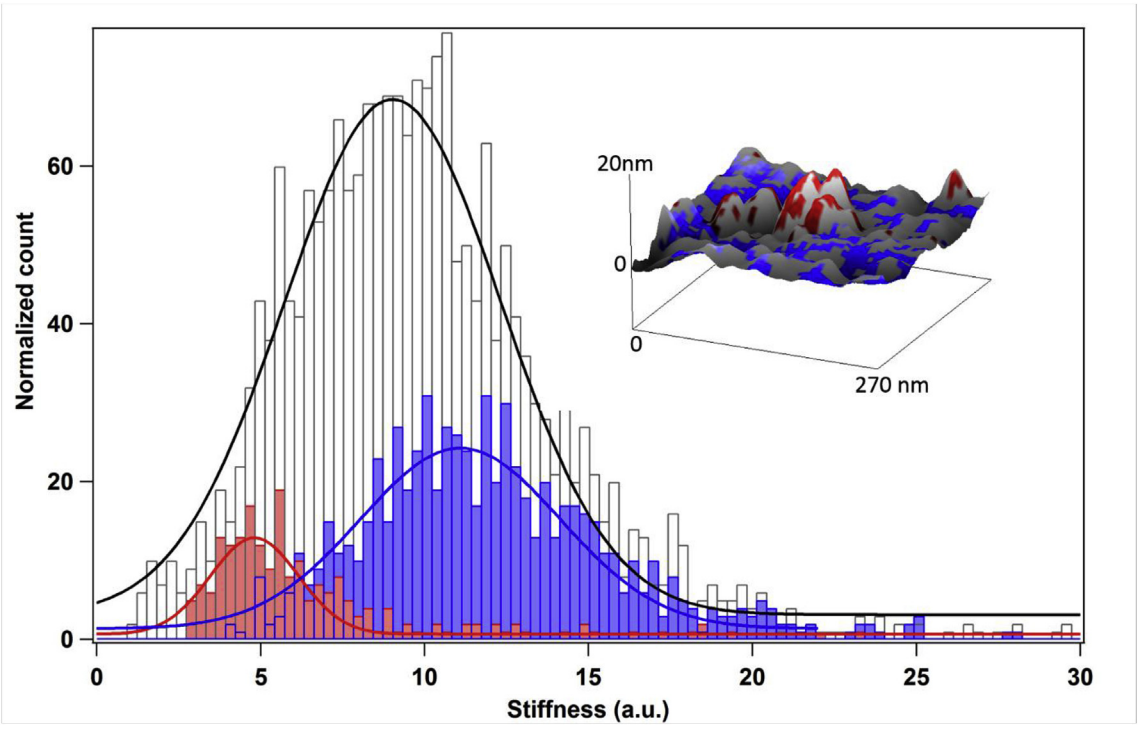

Fig. 3. Stiffness histogram from ImAFM measurements on EP/BNP15. The white bars show the histogram from the overall scanned area shown in the 3D topography including both particles and matrix. Blue bars are related to the stiffness histogram of epoxy phase (blue pixels on the 3D topography inset image) and red bars are related to stiffness BNPs (red pixels in the 3D topography inset image). Gaussian fits are shown as solid lines.

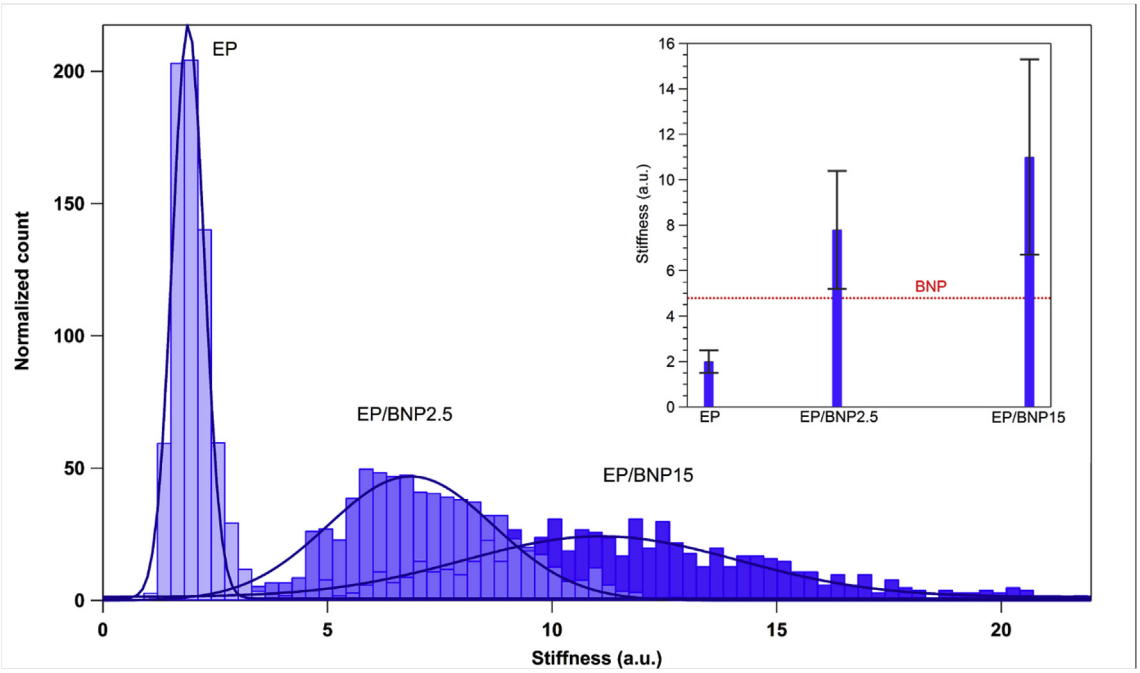

Fig. 4. Stiffness histogram from ImAFM of exclusively epoxy matrix, in EP/BNP2.5 and EP/BNP15 compared to neat epoxy EP. The inset plot compares the average stiffness values and the standard deviation are shown with error bars obtained from the gaussian fit (solid lines) of the stiffness histograms. The red dashed line in inset plot corresponds to the average stiffness value of BNPs in EP/BNP15 shown in Fig. 3.

of the matrix phase is no longer a constant but a variable of the particle concentration, theoretical micromechanical models such as Halpin-Tsai [28,29] fail to explain the behavior of this material. Comparison of experimental elastic modulus with Halpin-Tsai for various particle concentrations for EP/BNP15 is presented in supplementary material (SM2).

Since the ImAFM measurements are carried out at room temperature, the stiffness values qualitatively correlate to low-strain moduli of epoxy at glassy state. It is known that the glassy state moduli of epoxy systems are mainly related to chain interactions, intra- and intermolecular noncovalent bonding and intermolecular packing [30,31]. The decrease of crosslinking density results in better chain packings and thus increases the glassy state modulus. Thus, we hypothesize that the stiffening effect of BNPs on epoxy is due to inducing changes to crosslinking chemistry of epoxy and anhydride. the effect of BNPs on the crosslinking density of epoxy matrix is further investigated by applying dynamic mechanical analysis at elevated temperatures by evaluation of material response at glass transition and rubbery state.

3.2. DMTA measurements

DMTA measurements are performed to investigate the effect of BNP concentration on thermomechanical properties of EP/BNP nanocomposites and approximation of crosslinking density of epoxy matrix. All measurements are carried out on samples with 0, 1, 2.5, 5, 10 and 15 wt% boehmite content. The mechanical responses of nanocomposites were obtained as a function of temperature starting from the glassy state, through glass transition and reaching rubbery state. The temperature ramp was done twice for each sample, further referred as “first run” and “second run”. The modulus values obtained from only the first heating is comparable to stiffness values obtained from ImAFM and tensile modulus tests provided previously in literature [5,7,9]. Since samples experience elevated temperatures during the first DMTA ($T > T_g$), the results of second DMTA measurements are evaluated separately to demonstrate the effect of temperature treatment on thermomechanical properties of the nanocomposites.

3.2.1. Effect of BNP concentration (first run)

The storage shear modulus(G') and loss tangent ($tan\ \delta$) as function of temperature for samples with different particle concentrations are presented in Fig. 5.a and b, respectively. The storage modulus at glassy state is correlated to material stiffness under shear deformation. An increase in glassy state modulus with increase of BNP concentration is clearly observable (Fig. 5a). The same tendency was reported on static mechanical properties (tensile modulus) of similar composite systems [7].

However, in the rubbery state, the storage shear modulus shows a different behavior: the inset image of Fig. 5.a shows that for EP/BNP15 the storage modulus in the rubbery plateau drastically decreases. There is an approximation of crosslinking density based on theory of rubber elasticity, in which crosslinking density ν, is correlated to the storage shear modulus G' at rubbery plateau, R is the gas constant and T is the absolute temperature [32–34]:

$$G' = \nu RT \quad (1)$$

Eq. (1) is proposed for lightly crosslinked systems such as rubbers in which the elasticity is purely entropic, or the energy contribution of elasticity is negligible. In case of a highly crosslinked system with heterogenous phases consisting of nanoparticles, the intra- and intermolecular forces cannot be neglected and therefore the contribution of energetic elasticity needs to be considered. By taking energetic elasticity G_e into account, correlation between modulus G′ and crosslinking density ν can be approximated via Eq. (2) [35].

$$G' = G_e + \nu RT \quad (2)$$

As suggested by Pohl and coworkers [35], by extrapolating the rubbery plateau to absolute zero temperature, the axis intercept represents G_e which can have both negative or positive values. The slope of $G'(T)$ at rubbery state is taken as an approximation for ν.

G', ν and G_e values are calculated for nanocomposites with different particle contents and listed in Table 1. EP/BNP15 has the lowest crosslinking density while showing the highest modulus at glassy state. At first glance, the behavior of EP/BNP15 appears counterintuitive. However, as discussed before, the glassy state modulus is not correlated

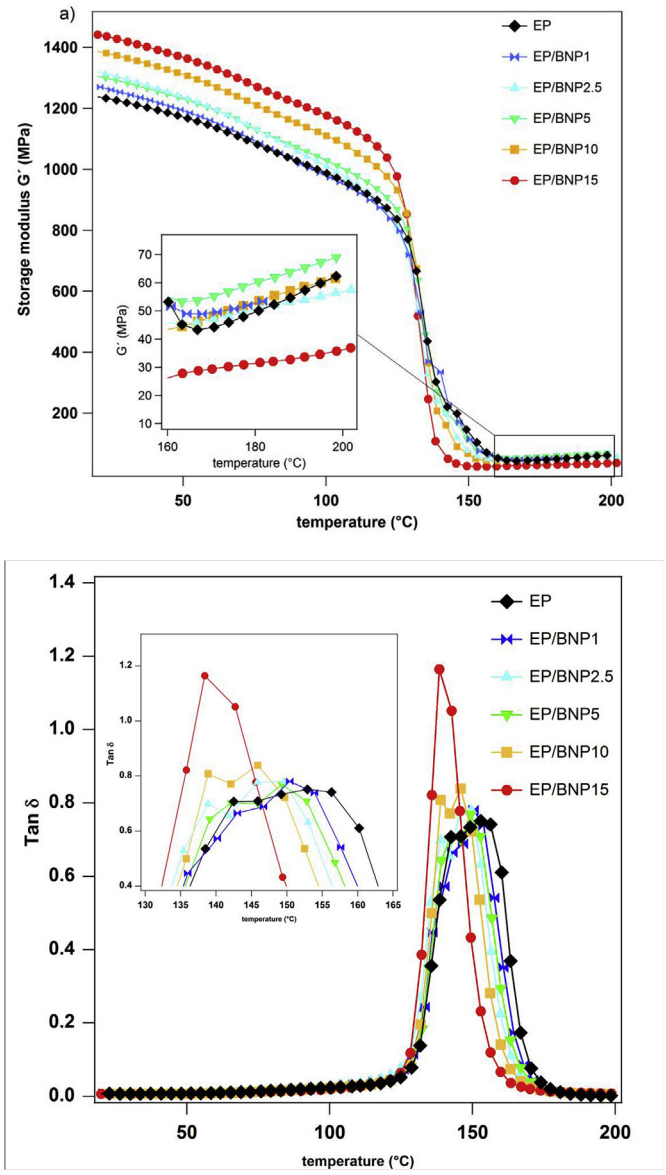

Fig. 5. a) storage shear modulus and b) loss tangent *tan* δ versus temperature for anhydride-cured epoxy nanocomposites EP/BNPs with different boehmite nanoparticle concentrations.

to crosslinking density. The glassy state modulus is mainly governed by non-covalent intra- or intermolecular interactions and intermolecular packing. In contrast, rubbery state modulus relates to the actual covalent crosslinks occur during the curing process. Here, the increase in glassy state modulus of the nanocomposite is partially related to the mechanical properties of particles. The other part is related to changes in the inherent properties of epoxy (as observed with ImAFM) which resulted in increase of intermolecular packing due existence of less covalent crosslinks and inter and intra-chain hydrogen bonding which may be caused by BNPs.

It is observed for all nanocomposites that G_e shifts to smaller values compared to unfilled epoxy, although no linear dependence to the particle concentration is observed. The magnitude of G_e shows its minimum at highest nanoparticle concentration (EP/BNP15). This comparison indicates that with high particle concentrations, following the argumentation of Pohl and coworkers, the response of the network at high temperatures is more entropy driven. According to the theory of rubber elasticity [32], an entropy driven network response is typical for rubbers, i.e. more lightly crosslinked networks. In lightly crosslinked networks, segmental chains have high mobility and less inter- and intramolecular forces compete with entropic elasticity. This means that in EP/BNP15, the matrix is comprised of a more lightly crosslinked network compared to unfilled epoxy.

The *tan δ* spectra obtained from the nanocomposites with different particle concentrations are presented in Fig. 5b. For the determination of the glass transition temperature T_g with DMTA, it is common to take either the maximum value of loss modulus or of *tan δ*. In this work the latter was chosen (the loss modulus spectra are presented in SM3.1). The analysis of *tan* δ, namely the position of peak maximum (T_g), peak height and width of half-height for each composition is presented in Table 1. It can be observed that T_g decreases with increasing BNP concentration. This is in the agreement with the trend observed in T_g values obtained from DSC [9]. Decrease of T_g is another indication of decreasing the crosslinking density [36].

The shape of *tan δ* peak including height and width also provides additional information about network structure. It is observed that besides T_g shift to lower values, *tan* δ peak also gets narrower with increasing BNP content. Broad *tan* δ peak indicates a wide distribution of molecular weight between crosslinks and therefore high heterogeneities of the network. The heterogeneous nature of cured epoxy were previously reported [24,37]. Kishi and coworkers attributed the heterogeneities to formation of local regions with low crosslinking densities [37]. Here, the bimodal peak observed for unfilled epoxy indicates that the polymer is a heterogeneous mixture of two distinguishable phases. As BNP content increases, the peak gets narrower and consequently a high sharp unimodal peak appears for 15wt% BNP content. Table 1 shows that for EP/BNP15, the width of half-height reduces up to 50% compared to EP. The sharp unimodal peak of EP/BNP15 shows that with high BNP concentration, the chemical network of epoxy becomes more homogenous although the crosslinking density is low. The changes in the height of *tan δ* peak for high particle concentration is also noteworthy. This value for EP/BNP15 shows approx. 60% increase compared to the height value in EP. The height of *tan δ* is associated with segmental mobility of network [31]. This implies that in EP/BNP15, polymer segments between crosslinks have higher mobilities which can be caused by formation of a network with lower crosslinking density compared to EP. Another reason can be the existence of high number of free chain ends in the network of EP/BNP15 or high number of unreacted monomer between the chains, which has higher mobility than the chains between crosslinks. Evidences on existence of a small

Table 1
Analysis of storage shear modulus, *tan* δ curves and the approximation of crosslinking density for each nanocomposite obtained from DMTA (first run).

composition	Storage modulus G' at room temperature (MPa)	Absolute value of energetic elasticity G_e (MPa)	Crosslinking density ν (mol m^{-3}) *10^6	Glass transition temperature T_g (°C)	Width of half-height (K)	Peak height (a.u.)
EP	1239	232	7.7	153	28	0.75
EP/BNP1	1270	111	7.3	150	25	0.78
EP/BNP2.5	1322	98	6.9	149	23	0.77
EP/BNP5	1307	163	8.7	149	23	0.78
EP/BNP10	1388	171	7.7	146	20	0.84
EP/BNP15	1442	69	4.4	140	14	1.17

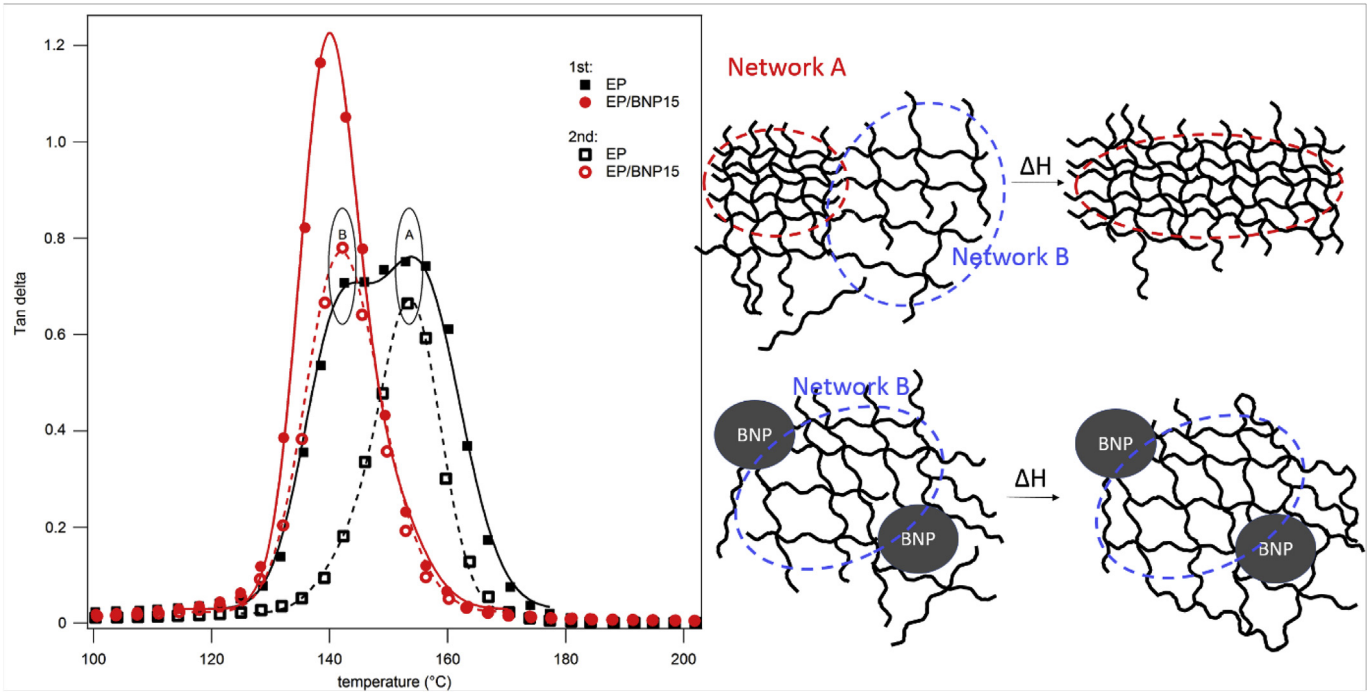

Fig. 6. Left: *tan* δ peak in first (filled red circles) and second (unfilled red circles) run of anhydride cured epoxy with 15wt% boehmite (EP/BNP15) shown with red marks compared with those of unfilled epoxy (EP) shown in black marks. The data point are fitted with double Gaussian distribution Right: simplified schematic of the effect of temperature on unfilled epoxy and EP/BNPs on the network topology of the epoxy.

fraction of unreacted monomers in EP/BNP with increasing BNP concentration has been observed with thermogravimetric analysis (see supplementary material, SM4).

3.2.2. Effect of temperature (second run)

So far, observations show that boehmite distorts the curing process and consequently alters the network density of epoxy, particularly at higher particle concentrations. The heterogeneous nature of epoxy network which appears as wide bimodal *tan δ* peak in the first run can be due to existence of segments which are not fully reacted. In this case it is expected that exposure to high temperatures during the first run causes an additional post-curing and consequently the matrix system will become more homogeneous with higher crosslinking density. Moreover, since boehmite has a higher thermal conductivity than epoxy, the question arises about the role of boehmite in the curing process by regulating the curing temperature. To investigate these effects, the second run DMTA measurements are evaluated and compared with the first run. The storage modulus *G′* and *tan δ* spectra obtained from the second run were quantitatively analyzed and presented in supplementary material (SM3.2 and SM3.3), respectively.

In Fig. 6, *tan δ* peak of EP and EP/BNP15 from the first run are compared to those from the second run. As mentioned before, the bimodal *tan δ* spectrum for EP is an indication of two segmental motions which represent two different network characteristics which we here call "*network A*" with T_g of 155 °C and "*network B*" with T_g of 141 °C. In the second run, the temperature affects the *network B* and what remains is the *network A* (T_g of 155°C). This indicates that EP went through additional curing during the first heating up. The network with low crosslinking density (*network B*) is hypothesized to be formed due to existence of non-covalently bonded segments of the network. During the DMTA measurement the material, for the first time after the preparation, experiences temperatures higher than its T_g. It seems that at temperatures higher than T_g, epoxy goes through a post-curing which leads to formation of additional chemical crosslinks and the network becomes homogeneous. The peak related to *network A* does not show any changes with exposure to high temperatures and hence this part of epoxy network has already reached its maximum crosslinking.

In the first run for EP/BNP15, *tan* δ peak is sharp and narrow, showing a maximum value close to that of the *network B* observed in EP. In the second run, unlike the neat epoxy, for EP/BNP15 the maximum and the width of the peak remains constant. It is expected that the low-crosslinked network of EP/BNP15 goes through the same post-curing as observed for *network B* in EP. However, based on these observations, EP/BNP15 has already reached its maximum crosslinking density during the preparation and further at elevated temperatures, no major crosslinking occurs. According to TGA-MS measurements shown in supplementray material (SM4), there is a larger number of unreacted anhydrides and DGEBA monomers in EP/BNP15 compared to EP. Although the mobility of these unreacted species increases at elevated temperatures, they are confined by the presence of large particles, thus the participation in further polymerization and formation of network is less possible for the confined monomers. Based on TGA measurements, at temperatures higher than 150 °C, the unreacted anhydride molecules desorb from the material, decreasing the chances of post-curing.

4. Discussion

We observed that BNPs induce changes in the epoxy matrix which lead to increase in stiffness of bulk matrix at room temperature (glassy state) while the network density is decreased. At first glance, this seems counterintuitive. However, a number of studies have demonstrated that in epoxy systems, the low strain modulus in glassy state is predominately correlated with intramolecular hydrogen bonding, free volume and intermolecular packing, while crosslinking density is the main factor of mechanical behavior at rubbery state [30,31,38]. Therefore, the mechanism behind the behavior in these two regions must be addressed separately.

Generally, three different mechanisms are proposed for the effect of particles on the curing behavior of epoxy [11]: 1) particles with higher thermal conductivity than the polymer, function as a temperature regulator within the matrix and consequently the curing behavior is changed. 2) Particles disturb the polymer network due to steric

limitations which results in decrease of crosslinking density. 3) Due to attractive forces between particles and matrix, the mobility of polymer chains are restricted which results in changes in curing by local alteration of stoichiometric ratio of resin and the hardener in the curing mixture in different distances from the particle. Here we discussed these three possibilities:

Since boehmite has a higher thermal conductivity than epoxy, it was proposed that BNP affects the curing process by homogenizing the temperature in the reaction volume. However, the comparison between the first and second runs of DMTA measurements, shows that temperature treatment influences the post-curing of epoxy in a significantly different way than introducing BNPs. While boehmite decreases the crosslinking density of the epoxy, exposure to high temperatures results in increase of crosslinking density. Therefore, the effect of boehmite as a temperature regulator is insufficient to describe the mechanical behavior and crosslinking density of anhydride-cured epoxy nanocomposite.

The increase in the number of unreacted monomers of epoxy and hardener with increasing the BNP content was observed with TGA-MS. Therefore, it is probable that BNPs decrease the crosslinking density of epoxy by sterically hindering diffusivity of monomers during the curing process. The steric hindrance of crosslinking by particles is a physical phenomenon which is related to the size and structure of particles and polymer. Therefore, it is expected to be observed in all boehmite-epoxy nanocomposites. However, in other studies on BNP/epoxy nanocomposites with a different curing agent, different behaviors were reported [39,40]. The DMTA results in these studies showed that neither T_g nor the crosslinking density was decreased. In some cases, the opposite effect was reported. It is clear, that the contradictory observation between these reports and observations in this study is due to chemical and physical interaction between BNPs and the matrix components especially the hardener. Therefore, in addition to sterically hindering the diffusion of monomers within the curing volume, the decrease of crosslinking density can be due to preferential absorption of anhydride on the surface of BNPs. This preferential absorption can lead to covalent bonding or hydrogen bridging between the carbonyl and hydroxyl groups. The evidences of strong interaction between BNPs and anhydride will be published elsewhere [41]. Another consequence of BNP-anhydride interaction is formation of phase segregation near the BNP interphase which was observed and published elsewhere [26]. This results in less reactive groups of anhydrides to be available for epoxy to react with. Therefore, the unbalanced stoichiometric ratio is expected to result a reduced crosslinking density.

5. Conclusion

Local nanomechanical properties of anhydride-cured epoxy/boehmite nanocomposite has been evaluated using ImAFM. The high resolution of this method allowed us to compare the stiffness of epoxy matrices in samples with different amount of nanoparticles by precisely distinguishing the force curves related to nanoparticles and polymer. It was observed that boehmite nanoparticles (BNPs) have significant long-range stiffening effect on bulk epoxy matrix in which the stiffness increases with increasing particle concentration. At higher concentrations of BNP, the stiffening effect of epoxy is in such an extent that the stiffness value of epoxy can locally exceed the stiffness of particles resulting in an inverse configuration in which particles act as plasticizer for the stiff matrix. The stiffening effect of BNP on epoxy is hypothesized to be due to alteration of network density during the curing process as a result of strong particle-polymer interactions. Using DMTA, investigations on crosslinking density of epoxy network in the presence of BNPs were carried out by evaluating the loss tangent peak characteristics and the rubbery state modulus. It was revealed that at high nanoparticle concentrations (15wt%), T_g and consequently the crosslinking density of epoxy decreases significantly. The stiffnened matrix together with contribution of the modulus of nanoparticles results in total enhancement of modulus of this nanocomposite compared to unfilled epoxy. Meanwhile in 15wt% nanocomposite, a looser network with higher mobility of segmental chains together with existence of unreacted monomers results in significant increase of fracture toughness and hinderance of crack propagation. The second run DMTA reveals that meanwhile the unfilled epoxy does not reach its maximum crosslinking by the suggested curing temperature program, the network density and T_g of 15wt% nanocomposite does not show a conciderable change during the temperature cycles, which indicates that the maximum crosslinking for this composition can be reached with lower curing temperatures.

Based on evidences in this work and an ongoing investigations on chemical interactions between boehmite nanoparticles, epoxy resin and the anhydride hardener, we suggest a mechanism for nanoparticle-polymer interaction in epoxy-boehmite nanocomposites which explains the decrease of crosslinking density meanwhile the increase of stiffness of matrix: The high number of hydroxyl groups on the surfaces of boehmite results in absorbtion of anhydride hardener (MTHPA) on the surface of nanoparticles via hydrogen or covalent bonding. Thus the curing chemistry of epoxy will be affected by i) promoting a different polymerization pathway by initiation of hydroxyl groups [42] ii) changes in stoichiometric ratio of hardener and epoxy and consequently formation of a network with different architecture (lower crosslinking density). An epoxy network which is loosely crosslinked due to chemical and physical interference of BNPs is able to form higher number of intra- and intermolecular noncovalent bondings and enhance the chain packings, resulting in higher stiffness compared to a highly crosslinked epoxy network. The local chemical composition of epoxy matrix and interphase using AFM-IR techniques, the interaction between boehmite and epoxy mixture components and a systematic study on mechanical properties of networks with varied stochiometric ratio are subjects of further studies.

Acknowledgement

The work is funded by German Research Foundation (DFG) in the frame of a research unit FOR2021: “Acting principles of nano-scaled matrix additives for composite structures”. Furthermore, the authors gratefully acknowledge Maximiliam Jux at Technical University of Braunschweig for preparation of the nanocomposite samples and Johannes Fankhänel for theoretical discussions. The authors especially wish to thank Petra Fengler for assisting with DMTA measurement and to Mrs. Sigrid Benemann for the SEM measurements. The authors also want to express their gratitude to Prof. Andreas Schönhals and Dr. Omid Zabihi for fruitful discussions.

Appendix A. Supplementary data

Supplementary data to this article can be found online at https://doi.org/10.1016/j.polymer.2018.12.054.

References

[1] T. Kruckenberg, R. Paton, Resin Transfer Moulding for Aerospace Structures, Springer Science & Business Media, 2012.
[2] C. May, Epoxy Resins: Chemistry and Technology, CRC press, 1987.
[3] B.C. Kim, S.W. Park, Fracture toughness of the nano-particle reinforced epoxy composite, Compos. Struct. 86 (1–3) (2008) 69–77.
[4] J. Karger-Kocsis, L. Lendvai, Polymer/boehmite nanocomposites: a review, J. Appl. Polym. Sci. 135 (24) (2017).
[5] C. Arlt, Wirkungsweisen nanoskaliger Böhmite in einem Polymer und seinem Kohlenstofffaserverbund unter Druckbelastung, Otto-von-Guericke Universität Magdeburg, 2011.
[6] M. Jux, et al., Effects of Al (OH) O nanoparticle agglomerate size in epoxy resin on tension, bending, and fracture properties, J. Nanoparticle Res. 19 (4) (2017) 139.
[7] M. Jux, et al., Mechanical properties of epoxy/boehmite nanocomposites in dependency of mass fraction and surface modification-An experimental and numerical approach, Polymer (2018).
[8] Z. Wu, et al., Mechanical properties of epoxy resins reinforced with synthetic

boehmite (AlOOH) nanosheets, J. Appl. Polym. Sci. 132 (5) (2015).
[9] W. Exner, et al., Nanoparticles with various surface modifications as functionalized cross-linking agents for composite resin materials, Compos. Sci. Technol. 72 (10) (2012) 1153–1159.
[10] N. Shahid, R.G. Villate, A.R. Barron, Chemically functionalized alumina nanoparticle effect on carbon fiber/epoxy composites, Compos. Sci. Technol. 65 (14) (2005) 2250–2258.
[11] K.W. Putz, et al., Effect of cross-link density on interphase creation in polymer nanocomposites, Macromolecules 41 (18) (2008) 6752–6756.
[12] L.E. Nielsen, Cross-linking–effect on physical properties of polymers, J. Macromol. Sci., Part C 3 (1) (1969) 69–103.
[13] C.D. Wood, et al., Understanding competing mechanisms for glass transition changes in filled elastomers, Compos. Sci. Technol. 127 (2016) 88–94.
[14] O. Zabihi, M. Aghaie, K. Zare, Study on a novel thermoset nanocomposite form DGEBA–cycloaliphatic diamine and metal nanoparticles, J. Therm. Anal. Calorim. 111 (1) (2013) 703–710.
[15] O. Zabihi, M. Ahmadi, M. Naebe, One-pot synthesis of aminated multi-walled carbon nanotube using thiol-ene click chemistry for improvement of epoxy nanocomposites properties, RSC Adv. 5 (119) (2015) 98692–98699.
[16] M. Abdalla, et al., The effect of interfacial chemistry on molecular mobility and morphology of multiwalled carbon nanotubes epoxy nanocomposite, Polymer 48 (19) (2007) 5662–5670.
[17] Z. Wang, et al., Controlled network structure and its correlations with physical properties of polycarboxyl octaphenylsilsesquioxanes-based inorganic–organic polymer nanocomposites, RSC Adv. 2 (7) (2012) 2759–2767.
[18] P.B. Messersmith, E.P. Giannelis, Synthesis and characterization of layered silicate-epoxy nanocomposites, Chem. Mater. 6 (10) (1994) 1719–1725.
[19] D. Platz, et al., Intermodulation atomic force microscopy, Appl. Phys. Lett. 92 (15) (2008) 153106.
[20] J. Fankhänel, et al., Mechanical properties of boehmite evaluated by atomic force microscopy experiments and molecular dynamic finite element simulations, J. Nanomater. 2016 (2016).
[21] J.L. Hutter, J. Bechhoefer, Calibration of atomic-force microscope tips, Rev. Sci. Instrum. 64 (7) (1993) 1868–1873.
[22] D. Platz, et al., Interaction imaging with amplitude-dependence force spectroscopy, Nat. Commun. 4 (2013) 1360.
[23] V.D. Hodoroaba, S. Rades, W. Unger, Inspection of morphology and elemental imaging of single nanoparticles by high-resolution SEM/EDX in transmission mode, Surf. Interface Anal. 46 (10–11) (2014) 945–948.
[24] J. Chung, M. Munz, H. Sturm, Amine-cured epoxy surface morphology and interphase with copper: an approach employing electron beam lithography and scanning force microscopy, J. Adhes. Sci. Technol. 19 (13–14) (2005) 1263–1276.
[25] K. Dušek, Are cured thermoset resins inhomogeneous? Angew Makromol. Chem.: Appl. Macromol. Chem. Phys. 240 (1) (1996) 1–15.
[26] M. Ghasem Zadeh Khorasani, et al., Insights into nano-scale physical and mechanical properties of epoxy/boehmite nanocomposite using different AFM modes, Polymers (2019) (submitted).
[27] H. Huang, Local Surface Mechanical Properties of PDMS-Silica Nanocomposite Probed with Intermodulation AFM, (2017).
[28] J. Halpin, Stiffness and expansion estimates for oriented short fiber composites, J. Compos. Mater. 3 (4) (1969) 732–734.
[29] Y. Zare, Development of Halpin-Tsai model for polymer nanocomposites assuming interphase properties and nanofiller size, Polym. Test. 51 (2016) 69–73.
[30] V. Gupta, et al., The temperature-dependence of some mechanical properties of a cured epoxy resin system, Polym. Eng. Sci. 25 (13) (1985) 812–823.
[31] H. Ishida, D.J. Allen, Mechanical characterization of copolymers based on benzoxazine and epoxy, Polymer 37 (20) (1996) 4487–4495.
[32] M. Rubinstein, R.H. Colby, Polymer Physics vol. 23, Oxford University Press, New York, 2003.
[33] M. Sharifi, et al., Toughened epoxy polymers via rearrangement of network topology, J. Mater. Chem. A 2 (38) (2014) 16071–16082.
[34] G. Levita, et al., Crosslink density and fracture toughness of epoxy resins, J. Mater. Sci. 26 (9) (1991) 2348–2352.
[35] G. Pohl, H. Goering, D. Joel, On the determination of network density in polyurethanes, Plaste Kautsch. 30 (4) (1983) 196–200.
[36] A. Seidel, Characterization and Analysis of Polymers, John Wiley & Sons, 2008.
[37] H. Kishi, et al., Mechanical properties and inhomogeneous nanostructures of dicyandiamide-cured epoxy resins, J. Polym. Sci. B Polym. Phys. 45 (12) (2007) 1425–1434.
[38] N. Amdouni, et al., Epoxy networks based on dicyandiamide: effect of the cure cycle on viscoelastic and mechanical properties, Polymer 31 (7) (1990) 1245–1253.
[39] M. Sangermano, et al., Epoxy-boehmite nanocomposites as new insulating materials, J. Appl. Polym. Sci. 114 (4) (2009) 2541–2546.
[40] A. Kyritsis, et al., Polymer dynamics in epoxy/alumina nanocomposites studied by various techniques, J. Appl. Polym. Sci. 121 (6) (2011) 3613–3627.
[41] M. Ghasem Zadeh khorasani, et al., Interphase Investigations on 2-D Model Sample of Epoxy-Boehmite Nanocomposite Using AFM-Based Approaches, (2018) (to be published).
[42] M. Morell, et al., New improved thermosets obtained from DGEBA and a hyperbranched poly (ester-amide), Polymer 50 (23) (2009) 5374–5383.